Air Quality, Atmosphere & Health (2018) 11:601–610
https://doi.org/10.1007/s11869-017-0542-4

Potential local and regional impacts of particulate matter emitted from one of the world's largest open-pit coal mines

Roberto E. Rojano[1,2] · Carlos A. Manzano[3] · Richard A. Toro[3] · Raul G. E. S. Morales[3] · Gloria Restrepo[2] · Manuel A. G. Leiva[3]

Received: 27 August 2017 / Accepted: 20 December 2017 / Published online: 12 January 2018

Abstract

This study was designed to evaluate the atmospheric total suspended particle (TSP) and particulate matter (PM_{10}) concentrations and temporal variability in one of the world's largest open-pit coal mines (El Cerrejon) located in northeast Colombia, during 2012–2016. The results showed overall average TSP and PM_{10} concentrations of 86 μg m^{-3} ($CI_{95\%}$ 84–88 μg m^{-3}) and 34 μg m^{-3} ($CI_{95\%}$ 33–35 μg m^{-3}), respectively, with the highest concentrations between March and August each year. A time trend analysis of the results revealed that PM_{10} concentrations in particular have significantly increased between 6.2 and 7.7% per year ($CI_{95\%}$ 1.2–12.8% year^{-1}) in several of the monitoring stations. Meteorological parameters were also evaluated. It was observed that NE winds with speeds above 2 m s^{-1} were significantly correlated with an increase in the concentration of PM_{10} for selected downwind sites, which suggested that coal mining operations are an important source of atmospheric PM in the area. Regional long-range atmospheric transport scenarios showed potential effects on neighboring municipalities and countries within 72-h transportation events. These highlighted the need to develop new strategies to control the emissions of PM from the local mining industry to comply with local and international guidelines and regulations, particularly when industrial expansion is planned for the near future and relatively large population centers are in the area, of which a high proportion belong to indigenous populations.

Keywords Particulate matter · Open-pit mining · Temporal trends · Cerrejon · Colombia · Long-range atmospheric transport

Introduction

Coal, oil, and natural gas are the main forms of fossil fuels. According to the World Coal Institute (WCI), there are over 984 billion tonnes of proven coal reserves distributed on every continent and recoverable with current technologies, enough to last for over 190 years (WCI 2005). Ten countries accounted for over 93% of the world total coal production in 2015: China (48%), the USA (12%), India (7%), Australia (7%), Indonesia (6%), Russian Federation (5%), South Africa (4%), Colombia (2%), Poland (1%), and Germany (1%) (BP 2016). Most of the production is destined to the electricity generation sector (~ 59% of the world total in 2012), the industrial sector (~ 36%), and residential/commercial consumption (~ 4%) (EIA 2017). According to the reference case of the U.S. Energy Information Administration (EIA) international energy outlook, coal will remain as the second largest energy source worldwide until 2030, with an average increasing consumption of 0.6% per year (EIA 2017).

Depending on the geology of the deposits, coal can be mined using surface (i.e., open-pit mining), or underground mining. Although underground mining currently accounts for over 60% of the world coal production (WCI 2005), open-pit mining accounts for 67–80% of the total production for some coal producers such as Australia, the USA, and Colombia

The names of 3 authors were incorrectly presented in the original article. Richard Toro A., Raul G. E. Morales S., and Manuel A. Leiva G. should Richard A. Toro, Raul G. E. S. Morales and Manuel A. G. Leiva.

Electronic supplementary material The online version of this article (https://doi.org/10.1007/s11869-017-0542-4) contains supplementary material, which is available to authorized users.

✉ Manuel A. G. Leiva
manleiva@uchile.cl

1 Grupo de Investigación GISA, Facultad de Ingeniería, Universidad de La Guajira, Km 5 Vía a Maicao, Riohacha, Colombia

2 Grupo Procesos Fisicoquímicos Aplicados, Facultad de Ingeniería, Universidad de Antioquia SIU/UdeA, Calle 70 No. 52-21, Medellín, Colombia

3 Centro de Ciencias Ambientales y Departamento de Química, Facultad de Ciencias, Universidad de Chile, P.O. Box 653, Santiago, Chile

(WCI 2005). Colombia ranked eighth in coal production in 2015 with proven reserves of 6746 million tonnes (BP 2016), most of which are located over its Atlantic coast in the region of La Guajira, including one of the largest coal open-pit mines in the world: Explotacion Cerrejon (ExCer) (Fig. 1, Online Resource 1: Fig. S1).

Large open-pit mines such as ExCer require the layer of soil, rocks, and vegetation covering the coal seams to be removed, which constitutes an additional source of atmospheric particulate matter (PM) to the known emissions from wind erosion, diesel exhaust from mining and transportation equipment, and haul roads (Chaulya 2004; Ghose and Majee 2007; Manzano et al. 2017). More than 82,000 tons of explosives per year is used for blasting operations at ExCer to remove over 225 million m^3 of overburden per year (Cerrejon 2016). The resulting material is then transported by haul trucks (with a capacity of 190–320 tons) to storage piles or processing units after which is transported via railroad (150 km) to the coastal city of Puerto Bolivar (the most important coal terminal in Latin America) for export mainly to Europe and North America (Cerrejon 2016). During the process, the material is leveled, wetted using water spraying and chemical additives, and compacted as a way to reduce dust emissions during the transportation (Cerrejon 2016), according to what have been described as effective strategies for dust control (Chaulya 2004; Ghose and Majee 2001). It has been estimated that these techniques can have a reduction of fugitive dust of as much as 88.6% in ExCer conditions (Rojano 2015). Previous studies have established that fugitive dust particles generated during open-pit mining can be an important contributor for total particles measured in ambient air (George et al. 2013; Ghose and Majee 2007; Manzano et al. 2017), and dust generated during coal mining has been associated with unique lung diseases such as coal worker's pneumoconiosis or progressive massive fibrosis (Finkelman et al. 2002).

In general, atmospheric PM is a concern, due to its harmful impacts on public health (Kim et al. 2015; Leiva et al. 2013), its influence on local climate (Buseck et al. 2000; Song et al. 2014), and its ecological impacts (Grantz et al. 2003). The total residence time of PM in the atmosphere differs from seconds to weeks, depending on the particle aerodynamic diameter. The residence time for the fraction of coarse particles ranges from hours to a few days and is determined by the equilibrium between sedimentation and turbulent mixing in the atmospheric boundary layer (National Research Council N 2010). As a consequence, PM_{10} generated in industrial locations, such as ExCer, can be subjected to regional atmospheric transport (Oh et al. 2015; Querol et al. 2004; Salvador et al. 2016; Xin et al. 2016). Therefore, a better understanding of PM sources, composition, distribution, and fate is needed, particularly for vulnerable population living close to PM sources.

It has been estimated that an increase of 10 μg m^{-3} in PM_{10} concentrations can lead to a 6% increase in mortality with 25,000 new cases of chronic bronchitis in adults and 290,000 in children, over 500,000 asthma attacks, and 16 million person-days of restricted activities in Austria, France, and Switzerland (Kunzli et al. 2000). According to the World Health Organization (WHO), the total number of premature deaths attributed to PM exposure was about 348,000 in 25 countries (WHO 2006).

ExCer has been declared as a nonpoint source of atmospheric pollution by the Colombian Government, and total

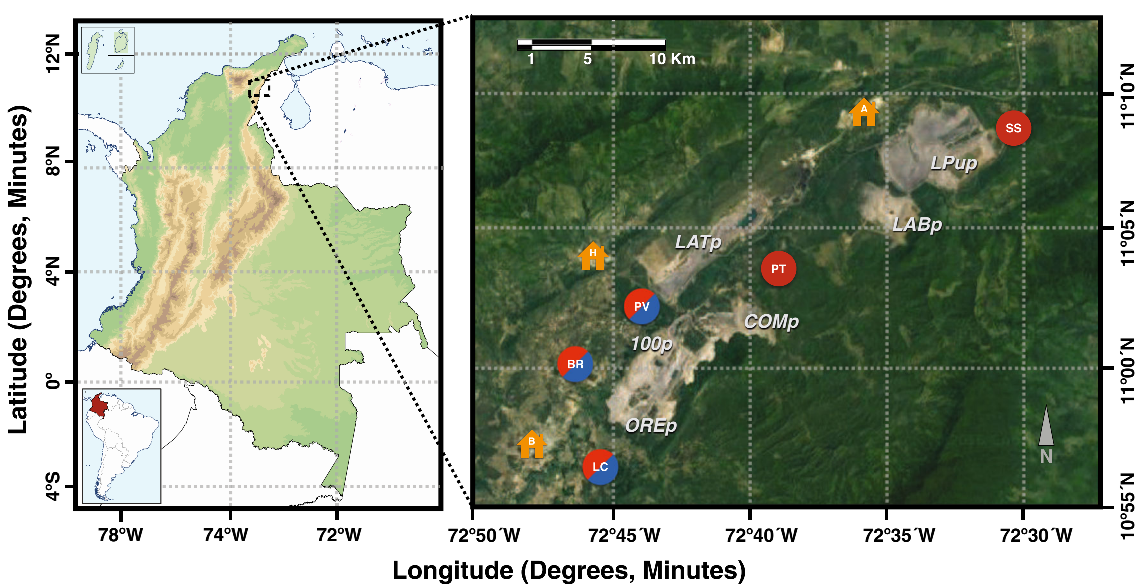

Fig. 1 Geographic location of ExCer and selected sampling sites: BR (Barrancas), LC (Las Casitas), PT (Patilla), PV (Provincial), and SS (Sol y sombra). Nearby municipalities (B, Barrancas; H, Hatonuevo; and A, Albania) are also shown. Left panel: modified from Mapa de Colombia (orografía).svg Wikipedia, https://goo.gl/Wg6TzI, accessed 2016-03-02; right panel source: Google earth v7.1.5.1557, 2016-03-02, DigitalGlobe 2016. http://www.earth.google.com, accessed 2017-03-10).

suspended particle (TSP) and PM_{10} are constantly monitored in the area. This study was designed to evaluate the concentrations of TSP and PM_{10} and temporal variability in selected monitoring stations from the ExCer air quality monitoring network in northern Colombia during 2012–2016. Meteorological parameters and potential long-range transport properties were also evaluated. The results were compared with other similar industrial sites worldwide and can be used to design new strategies to control and contribute to resolve the air quality problem in the area.

Materials and methods

Study site

The study was conducted at the main ExCer coal mine developments (11° 5′ 2″ N; 72° 40′ 31″ W) in the Colombian Atlantic Coast, region of La Guajira. ExCer currently has an approximated area of 800 km^2 with an extractive capacity of over 30 million tonnes (Mt) of coal per year (42 Mt projected production for 2016), representing ~41% of the total Colombian exports (Cerrejon 2016) (Fig. 1).

The projected 2016 population for the entire region of La Guajira in the Atlantic region of Colombia reaches 957,797 (DANE 2005). ExCer is located close to relatively large population centers in the region, such as Riohacha (capital of the region of La Guajira), and Barranquilla (the largest industrial center in the region) located 100 and 400 km away from ExCer, respectively. Currently, over 40,000 people live within 10 km of ExCer, in the municipalities of Barrancas, Hatonuevo, and Albania (Fig. 1), 34% of which correspond to indigenous groups (DANE 2005).

Sample collection

Five monitoring stations from the ExCer air quality and monitoring network were selected based on their locations to surround the six main exploitation areas (from north to south): Tabaco pit (TABp), La Puente pit (LPUp), Patilla pit (PATp), Comunero pit (COMp), 100 pit (100p), and Oreganal pit (OREp) (Fig. 1). The sites were located at the north (SS), center (PT, PV), and south (BR, LC) of the main ExCer developments (Fig. 1, Table 1), in order to evaluate potential downwind and upwind conditions.

TSP and PM_{10} samples were collected continuously from 2012 to 2016 using a TE-5170 and TE-6070 high-volume samplers (Hi-Vol), respectively, both purchased from Tisch Environmental (Cleves, OH, USA) equipped with 2-μm Whatman® glass- and quartz-fiber filters (8 × 10 in.), purchased from Sigma-Aldrich (St Louis, MO, USA). Samples were collected as 24-h samples every 3 days for TSP, and every 6 days for PM_{10} for a total of 2226 TSP samples and 1762 PM_{10} samples.

All samples were processed and analyzed for TSP and PM_{10} using gravimetrical techniques, following reference methods of the Code of Federal Regulations (Appendix B to Part 50 for TSP and Appendix J to Part 50 for PM_{10}) (EPA 1999, 2011). The filters were prepared in the Center for Air Resources Engineering and Science (CARES) at Clarkson University, packaged and shipped to Colombia. Briefly, each filter was conditioned to 30 ± 10% relative humidity, and 20 ± 2 °C for 24 h and stored at 4 ± 2 °C prior and after deployment until 2 h before the analysis. The weight difference between the clean and exposed filters was then recorded using an EX125D Ohaus analytical balance (Paisippany, NJ, USA) with a 0.01 mg accuracy.

Additionally, meteorological variables, such as temperature (*T*), relative humidity (RH), precipitation (Pp), wind speed (ws), and wind direction (wd), were obtained from three of the selected sampling sites (i.e. PV, BR, and LC).

Data analysis

Data analysis was completed using Microsoft Excel® 2016 (Microsoft Corp., Redmond, WA), and R-Studio (www.rstudio.org, Boston, MA) using the air quality tool "OpenAir" (Carslaw and Ropkins 2012). The correlation between meteorological variables and TSP and PM_{10} concentrations was evaluated using Pearson coefficients, while the effect of wind direction and speed was evaluated using R-studio and the polarPlot tool (Carslaw and Ropkins 2012). The Sen-Theil estimator was used to explore the temporal variability of the data obtained from all sites during 2012–2016, and to estimate future scenarios.

Table 1 Selected sampling sites from ExCer air quality and monitoring network, their geographical coordinates and elevation above sea level (m)

Site ID	Site name	Lat	Long	Elevation (m)	Variables measured
SS	Sol y Sombra	11° 8′ 37.88″ N	72° 30′ 36.64″ W	117	TPS, PM_{10}
PT	Patilla	11° 30′ 00″ N	72° 40′ 15.60″ W	115	TPS, PM_{10}
PV	Provincial	11° 1′ 23.12″ N	72° 44′ 5.99″ W	156	TPS, PM_{10}, *T*, *P*, ws, wd
BR	Barrancas	10° 57′ 34.38″ N	72° 46′ 45.52″ W	150	TPS, PM_{10}, *T*, *P*, ws, wd
LC	Las Casitas	10° 57′ 1.69″ N	72° 44′ 28.23″ W	162	TPS, PM_{10}, *T*, *P*, ws, wd

All TSP and PM_{10} concentrations were compared to air quality standards set by the Colombian national air quality standards (NAQS: TSP and PM_{10} annual average concentrations of 100 μg m^{-3}—geometric mean—and 50 μg m^{-3}—arithmetic mean—and daily average concentrations of 300 μg m^{-3}—geometric mean—and 150 μg m^{-3}—arithmetic mean—respectively) (MADS 2010), international guidelines set by the World Health Organization (WHO: PM_{10} annual and daily average concentrations of 20 and 50 μg m^{-3}, respectively) (WHO 2006), and to other published studies for similar mining sites and urban centers.

Air mass trajectory analysis

The Hybrid Single Particle Lagrangian Integrated Trajectory (HYSPLIT), developed for computing air mass trajectories and complex dispersion and deposition simulations (Rolph et al. 2017; Stein et al. 2015), was used (MAC Version 4.8). A forward 72-h trajectory analysis was calculated four times per day (at 0, 6, 12, and 18 h, daily) for starting heights of 10 m, and from January 1, 2012 to December 31, 2016. A total of 7304 trajectories were calculated using global meteorological data from the National Center for Environmental Prediction and the National Center for Atmospheric Research (NCEP/NCAR). A frequency analysis of the trajectories generated was performed by activating the residence time option in HYSPLIT. Cluster analysis to group trajectories with similar paths was performed. The objective of clustering techniques is to maximize the homogeneity of elements (in our case, forward trajectories) within the clusters and also to maximize the homogeneity among the clusters. In this study, a non-hierarchical cluster analysis using the *k-means* method (Ashbaugh et al. 1985) was applied using the software MeteoInfo version 1.4.6R4 (Wang 2014), and the plug-in TrajStat version 1.4.4R8 with the angle distance algorithm (Wang et al. 2009). Additionally, an analysis of potential impact (PI), as described by Koçak et al. (2011), was performed for forward trajectories and using the average concentrations observed in the areas close to ExCer for concentrations greater than 20 μg m^{-3} (further details can be found in Online Resource 1: "Potential Impact model in HYSPLIT"). Finally, the resulting trajectories, cluster analysis, and PI were plotted using QGIS version 2.12.1-Lyon (QGIS 2016).

Results and discussion

ExCer characteristics

ExCer is located in a tropical semi-arid region. The local geography is shaped by the Rancheria River watershed, located between two mountain ranges (Perija to the east, and Sierra Nevada to the west) (Fig. 1), which results in coal deposits found at different depths (10–50 m for the most surface layers, and as deep as 200 m) and with thickness as much as ~ 10 m (ANLA 2015). Meteorological variables were measured at selected locations (sites PT, BR, LC) (Online Resource 1: Fig. S2.) and showed annual average temperatures of 29.5 °C (percentile 25%, Q1 = 28.1 °C; percentile 25%, Q3 = 30.7 °C), predominant ENE winds (frequencies ~ 30%) with average wind speed of 2.90 m s^{-1} (percentile 25%, Q1 = 2.00 m s^{-1}; percentile 25%, Q3 = 3.60 m s^{-1}), and high RH (average 65%; percentile 25%, Q1 = 59%; percentile 25%, Q3 = 70%) with an average annual precipitation of 400 mm with the driest period between January and February (ANLA 2015; CIOH 2010; Rojano et al. 2017). No significant differences among sites for each variable (ANOVA, $p > 0.05$) (Online Resource 1: Table S1). This suggested that there are uniform meteorological characteristics for the entire study area.

TSP and PM_{10} concentrations

The TSP and PM10 average concentrations showed a characteristic pattern of intra-annual variability (Fig. 2a), with periods of maxima and minima repeated throughout the years studied. The annual average (arithmetic) TSP concentrations for the period 2012–2016, considering all sampling sites, were 86 μg m^{-3} ($CI_{95\%}$ 84–88 μg m^{-3}); while the annual average (arithmetic) PM_{10} concentration was 34 μg m^{-3} ($CI_{95\%}$ 33–35 μg m^{-3}) (Online Resource 1: Table S2). This showed an overall 2.5-fold difference between TSP and PM_{10}. No inter-annual variability was observed for TPS and PM_{10} annual averaged concentrations in the sampling sites analyzed during 2012–2016 (ANOVA, $p > 0.05$) (Online Resource 1: Table S3).

Considering individual sites, the highest overall TSP annual average concentrations (arithmetic) during 2012–2016 were observed at site LC (111 μg m^{-3}; $CI_{95\%}$ 106–115 μg m^{-3}), followed by PV (100 μg m^{-3}; $CI_{95\%}$ 96–103 μg m^{-3}), PT (95 μg m^{-3}; $CI_{95\%}$ 91–98 μg m^{-3}), BR (87 μg m^{-3}; $CI_{95\%}$ 84–90 μg m^{-3}), and SS (41 μg m^{-3}; $CI_{95\%}$ 40–43 μg m^{-3}) (Online Resource 1: Table S2). Similarly, the highest PM_{10} annual average (arithmetic) concentrations were observed at site LC (41 μg m^{-3}; $CI_{95\%}$ 40–42 μg m^{-3}), followed by sites PV (38 μg m^{-3}; $CI_{95\%}$ 37–39 μg m^{-3}), BR (35 μg m^{-3}; $CI_{95\%}$ 33–36 μg m^{-3}), PT (34 μg m^{-3}; $CI_{95\%}$ 32–36 μg m^{-3}), and SS (23 μg m^{-3}; $CI_{95\%}$ 22–24 μg m^{-3}) (Online Resource 1: Table S2). Both PM and TSP showed an increase in concentrations following a NE-SW direction.

TSP and PM_{10} concentrations measured at the same sampling site were positively correlated (Pearson correlation coefficients, *r*, ranged from 0.72 to 0.82), suggesting a potential common source for both (Online Resource 1: Table S4). Additionally, a strong correlation was also observed when comparing TSP concentrations between all sites, except for

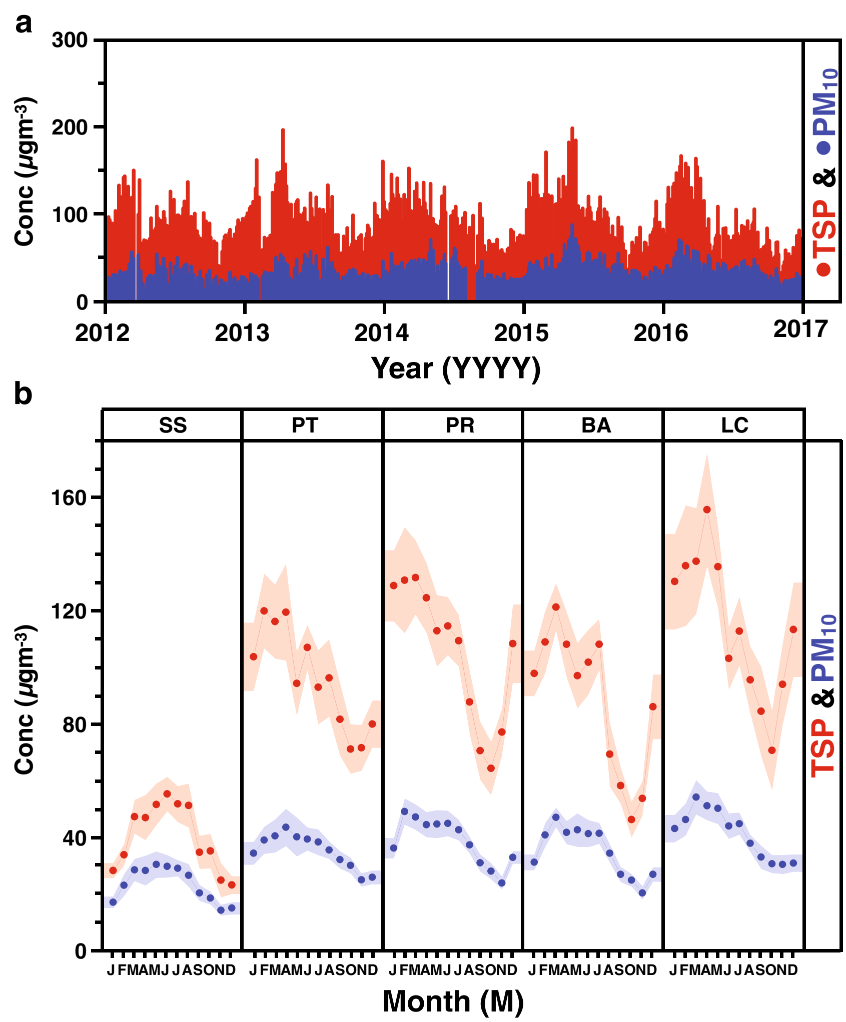

Fig. 2 **a** Time series of daily average TSP (in red) and PM_{10} (in blue) concentrations for all sampling sites selected during 2012–2016. **b** Monthly average TSP (in red) and PM_{10} (in blue) concentrations for all sampling sites during 2012–2016

SS (r ranged from 0.58 to 0.80); and PM_{10} concentrations between all sites (r ranged from 0.58 to 0.83), except for LC-SS, LC-PT, and PV-SS (Online Resource 1: Table S4). Site SS showed a different behavior particularly for TSP, with relatively low correlations between sites (r ranged from 0.10 to 0.33), suggesting that SS has different sources of TSP compared to other sites located downwind of ExCer, a major source of TSP and PM_{10}.

TSP and PM_{10} seasonality

Daily averaged (arithmetic) TSP and PM_{10} concentrations for 2012–2016 showed clear seasonal patterns, with higher concentrations for the first months of each year and higher TSP concentrations compared to PM_{10}, as expected (Fig. 2b). The monthly averaged TSP and PM_{10} concentrations between February and March were significantly greater than those observed between October and November (ANOVA, $p < 0.05$) (Online Resource 1: Table S3), for all sampling sites except SS (Fig. 2b). This overall trend can be explained by the precipitation patterns, which were higher during September–November with over 10 rainy days each month, that could decrease the atmospheric TSP and PM_{10} concentrations due to its scavenging effect. On the other hand, less frequent precipitation events were observed during January–July (with 2 days of precipitation each month), which can increase their atmospheric residence time.

Sampling site SS showed different patterns to all other sampling sites and showed the highest TSP and PM_{10} monthly concentrations observed during March to August, while the lowest concentrations were observed from September to February (Fig. 2b). The PM_{10} monthly averaged concentrations at site SS during February–June were significantly different than those observed during September–December (ANOVA, $p < 0.05$) (Online Resource 1: Table S3). Given that the recorded precipitation rate and average RH are similar throughout the sampling area, this reinforces the idea that SS had different TSP and PM_{10} sources. Site SS is located upwind of most of the industrial activities taking place at ExCer (> 30% wind frequencies in the area were from the NEE and

NE), thus reducing the impact of all PM generated during coal mine-related activities.

Meteorological factors

TSP and PM_{10} showed a negative correlation with RH (Pearson correlation coefficients, r, ranged from − 0.05 to − 0.31) and precipitation (r ranged from − 0.19 to − 0.25), and a positive correlation with temperature (r ranged from 0.15 to 0.31) (Online Resource 1: Fig. S3 and Table S5). Although the correlation coefficients observed were relatively low, the effects of relative humidity, precipitation, and temperature on atmospheric particles and their dry and wet deposition are well known (Lei and Wania 2004; White and Blum 1995).

Wind speeds are important factors in the study of atmospheric particulate matter, because they can affect particle dispersion and transport potential (Manzano et al. 2016; Molina et al. 2017). A positive correlation between wind parameters (wind speed) and TSP and PM_{10} concentrations was observed (r ranged from 0.20 to 0.61). OpenAir, with the polarPlot package, was used to further evaluate the interaction between TSP and PM_{10} concentrations and wind parameters. Higher TSP and PM_{10} concentrations were observed at wind speed conditions of over 2 m s^{-1}, with predominant winds from the NEE, NNE, and NE (Fig. 3). Sites LC and BR showed strong contributions from NNE, NE, and E winds particularly for wind speeds between 2 and 5 m s^{-1} (Fig. 3). The TSP and PM_{10} concentrations in the bivariate plot followed downwind directions, and the highest concentrations during 2012–2016 were observed in site LC, followed by BR and PV (Fig. 3). This indicated a direct impact of the mining activities of ExCer and its closest pits: PATq, 100p, and OREp. Alternatively, site PV showed stronger contributions of E winds with wind speed from 2 to 5 m s^{-1}, which can be related to a contribution from pits COMp and PATp. This reinforced the idea of local mining activities as the main source of atmospheric TSP and PM_{10}. However, emissions from coal mining industry could include diesel exhaust from mining and transportation equipment, haul roads, airborne particulate matter from mine and land disturbances, and also other natural sources such as forest fires. Further studies on the characterization and distribution of particulate matter collected from the area are needed for a comprehensive source apportionment.

Cluster analysis and potential impact at regional level

Regional meteorology may play an important role circulating the particles originating from ExCer and other sources. It is important to mention that it has been estimated that the residence time of the PM_{10} could range from days to weeks (Oh et al. 2015; Querol et al. 2004; Salvador et al. 2016; Xin et al. 2016); therefore, there is the potential for long-range regional transport. Figure 4a shows the HYSPLIT analysis for seven clusters (C) of direct trajectories with individual contributions of 29.2% (C_2), 23.7% (C_1), 17.6% (C_3), 1.42% (C_4), 12.10% (C_5), 15.07% (C_6), and 0.94% (C_7). The predominant clusters are represented by C_2, C_1, and C_3, which account for 70% of the total (Fig. 4a, Online Resource 1: Fig. S4). This suggested that the most likely areas to be affected by the emissions from ExCer are located in the WSW and SSW direction from the main mining developments. The trajectories indicated potential impacted areas in Colombia and southern Panama. A potential impact map for PM_{10} is presented in Fig. 4b. The results showed that the areas with the greatest impact are in the same direction as those indicated by the cluster analysis. The PI in Fig. 4b considers the PM residence time in the atmosphere and shows potential impacted areas (Fig. 4, Online Resource 1: Fig. S3). Further studies are needed in these locations to confirm the source of the PM collected. Additionally, $PM_{2.5}$ monitoring must be included to the already existent PM_{10} and TSP monitoring plans.

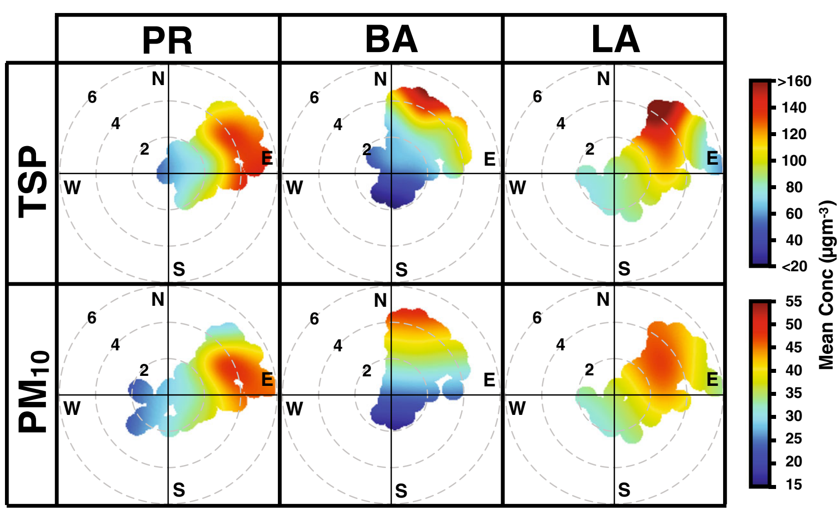

Fig. 3 Bivariate polar plot of PM_{10} and TSP concentrations (µg m^{-3}) at ExCer during 2012–2016, at sites PV, BR, and LC

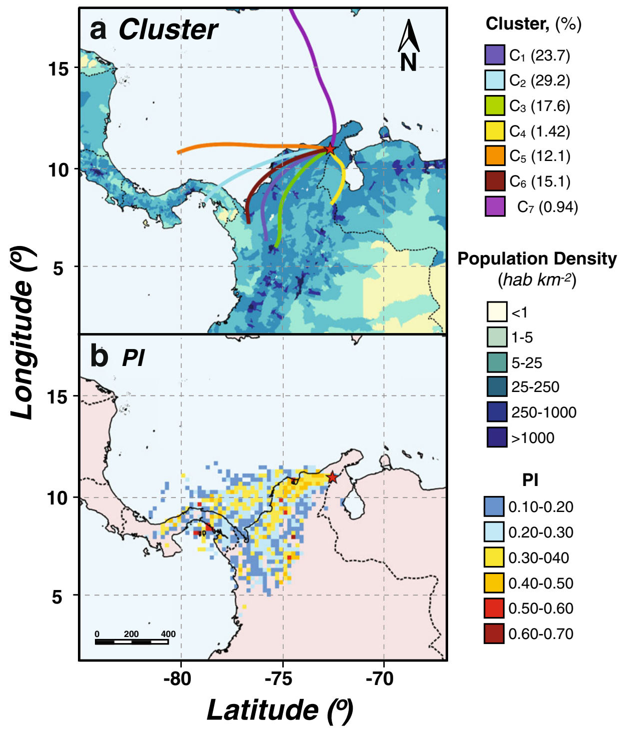

Fig. 4 **a** HYSPLIT cluster and frequency analysis results for 7304 forward 72-h air trajectories from 1/1/2012 to 12/31/2016 and population density. **b** Potential impact (PI), colors show the probability of finding high-concentration PM for the trajectories in **a**

TSP and PM_{10} trends

The Sen-Theil estimator, which uses the median of the slopes of all lines through pairs of two-dimensional sample points, was used to generate time trends for all sampling sites during 2012–2016. The method is robust with respect to outliers and can be significantly more accurate than simple linear regression for skewed data. The "de-season" option was used to remove the inter-annual variability of the data before performing the time trend analysis.

The estimated results showed no significant trends on TSP concentrations for sites BR, LC, and PT ($p > 0.1$), for which the estimated slopes include 0. Site PV showed a decrease in TSP concentration for 2012–2016 (slope −2.766, $p < 0.1$) (Online Resource 1: Table S6), which corresponds to a decrease of 2.7% per year. Alternatively, site SS showed an increase in TPS concentrations during 2012–2016 (slope 5.311, $p < 0.1$) that corresponded to a 5.3% increase per year.

PM_{10} showed increasing trends in concentration for sampling sites PT, BR, and SS ($p < 0.01$), with estimated slopes ranging from 6.2 to 7.7% per year (Online Resource 1: Table S6), and particularly high significance for sites BR and PT. Alternatively, sites LC and PV showed no significant trends ($p > 0.1$) (Online Resource 1: Table S6).

The estimated increase in TSP and PM_{10} measured in at least three of the five sampling sites from 2012 to 2016 is consistent with the historic increase of production in ExCer (from 2.2 Mt in 1985 to 42 Mt projected for 2016) (Cerrejon 2016), and with local changes in the area. For example, a new public road was open close to site SS in 2015, which can increase the emission of fugitive dust to this area. Other climatological factors such as El Nino Southern Oscillation phenomenon, which caused a decrease of rains in the area in 2015 and 2016, could also affect the measured TSP and PM_{10} values. Further analysis and monitoring programs must be implemented in the area to prevent further impact on local ecosystems and population health, which includes a high percentage of vulnerable groups (low socio-economic status and indigenous groups).

Air pollution assessment

TSP annual geometric mean concentrations exceeded NAQS guidelines (geometric mean 100 μg m^{-3}) at site PT in 2015 (106 μg m^{-3}), and at site LC in 2013 and 2015 (100–110 μg m^{-3}), while it was lower than NAQS at all times at sites PV, BR, and SS. Similarly, PM_{10} annual arithmetic mean concentrations were always below NAQS guidelines at all sites during 2012–2016. Colombian NAQS are in the same range of those found in other selected mining countries (Table 2). However, they are significantly lower than WHO guidelines and standards which are established for more residential contexts. The annual PM_{10} concentration measured exceeded WHO standards (20 μg m^{-3}, annual arithmetic mean) at all sites, and by as much as 25% at site LC. Similar results were observed with the WHO daily PM_{10} concentration standard (50 μg m^{-3}).

PM_{10} annual arithmetic mean concentrations measured at ExCer (17–42 μg m^{-3}) (Table 2) were within the concentration levels observed in other similar areas worldwide: Kozani, Greece (20–35 μg m^{-3}); Jharia coalfield, India (21–101 μg m^{-3}); Zonguldak, Turkey (12–200 μg m^{-3}); and Roda, VA, USA (19–219 μg m^{-3}), but were lower than other industrial sites: Lakhanpur, India (103–426 μg m^{-3}); Padmapur, Chandrapur, India (240 μg m^{-3}); and Pingdingshan, China (265–1066 μg m^{-3}) (Table 2). Other urban centers not directly related to coal show similar concentrations than those measured at ExCer: Buenos Aires, Argentina (26 μg m^{-3}); Sao Paulo, Brazil (35 μg m^{-3}); and Medellín, Colombia (45 μg m^{-3}), and are even lower than those observed in Caracas, Venezuela (47 μg m^{-3}); Bogotá, Colombia (52 μg m^{-3}); Santiago, Chile (64 μg m^{-3}); Lima, Perú (88 μg m^{-3}); and Beijing, China (108 μg m^{-3}) (Table 2).

TSP concentrations measured at ExCer (36–125 and 32–110 μg m^{-3}, annual arithmetic and geometrical mean concentrations, respectively) are also within measured values in residential zones from Jharia coalfield (93–452 μg m^{-3}) and

Table 2 Daily TSP and PM_{10} ambient air quality guidelines for selected countries, concentration ranges found in the literature and values measured in this study

	PM_{10} (μg m^{-3})	TSP (μg m^{-3})	Observation	Reference
Air quality standard				
Colombia	150*	300**	–	(MADS 2010)
USA	150*	–	–	(EPA 2017)
Australia	50*	–	–	(DEE 2008)
India (industrial)	150*	500*	–	(CPCB 2003)
India (residential)	100	200*	–	(CPCB 2003)
WHO	50*	–		(WHO 2006)
Comparison of studies around the world				
ExCer, Colombia (coal mine)	23–41*	37–98**	2012–2016 annual average, all sites	This study
Close to coal-fields or mines				
Jharia coalfield, India (work zone)	473–780	2201–3724	–	(Ghose and Majee 2007)
Jharia coalfield, India (ambient)	21–101	93–452	–	(Ghose and Majee 2007)
Ghugus, Wani, India (industrial)	372 *	–	–	(George et al. 2013)
Padmapur, Chandrapur, India (industrial)	240 *	–	–	(George et al. 2013)
Western Turkey (industrial)	1848 *	–	–	(Onder and Yigit 2009)
Lakhanpur, India (residential)	41–172	72–497	–	(Chaulya 2004)
Lakhanpur, India (industrial)	103–426	339–800	–	(Chaulya 2004)
Zonguldak, Turkey (residential)	12–200	–	–	(Tecer et al. 2008)
Roda, VA, USA (residential)	32–470	–	–	(Aneja et al. 2012)
Kozani, Greece (residential)	20–35	–	–	(Tolis et al. 2014)
Urban centers				
Buenos Aires, Argentina	26	–	2015; 3 stations, residential and commercial	WHO 2016
Sao Paulo, Brazil	35	–	2014, 24 stations,	http://www.who.int/phe/health_topics/outdoorair/databases/cities/en/
Medellin, Colombia	45	–	2014, 5 stations, urban/suburban background	
Caracas, Venezuela	47	–	2012, 2 station	
Bogota, Colombia	52	–	2014, 10 stations, urban background/urban traffic	
Santiago, Chile	64	–	2014, 10 stations	
Lima, Peru	88		2013, 5 stations	
Beijing, China	108	–	2013	

*Arithmetic mean

**Geometric mean

Lakhanpur, India (72–497 μg m^{-3}) and are significantly lower than those observed in the industrial zones of Lakhanpur (339–800 μg m^{-3}) and Jharia coalfield in India (2201–3724 μg m^{-3}) (Table 2).

Conclusions

The PM_{10} and TSP concentrations measured exceeded WHO international guidelines for daily and annual averages for most sites, but were mostly below Colombian national air quality standards. Three monitoring stations showed increasing trends in TSP and PM_{10} concentrations from 2012 to 2016.

TSP and PM_{10} concentrations measured at the same sites showed strong positive correlation, suggesting a common source for both at each site. Sampling site SS (located upwind from ExCer) showed different concentration profiles, suggesting that ExCer is an important contributor for all sites located downwind of the main developments. This was reinforced by the strong positive correlations observed for TSP and PM_{10} concentrations and wind direction, of which the highest TSP and PM_{10} concentrations were observed for NE winds with speeds > 2 m s^{-1}. Potential regional long-range transport of PM to central Colombia (south of ExCer) and southern Panama (west of ExCer) within 72 h was observed in the HYSPLIT modeling. However, further studies are needed to confirm the source of PM material found in these locations. The emission of fugitive dust particles from ExCer must be reduced and control by the implementation of effective mitigation strategies: restrictions of the loadings of trucks, speed limits, improve regular cleaning of roads, dust suppressive measures such as regular water spraying, biological reclamation, and green belts.

Acknowledgments The authors thank the logistic support of the University of Antioquia (Universidad de Antioquia), The University of La Guajira (Universidad de la Guajira) and the Center for Environmental Science at the Faculty of Science, University of Chile (Centro de Ciencias Ambientales, Facultad de Ciencias de la Universidad de Chile). The authors gratefully acknowledge the NOAA Air Resources Laboratory (ARL) for the provision of the HYSPLIT transport and dispersion model for MacOS version (http://www.ready.noaa.gov) used in this publication. Data will be made available on request.

Funding information RER acknowledges partial support of Colciencias-Cerrejón joint program, Grant No. 1115-524-30465. MALG acknowledges support of National Commission for Scientific and Technological Research CONICYT/FONDECYT 2016 grant no. 1160617.

Compliance with ethical standards

Competing interests The authors declare that they have no competing interests. The funders had no role in study design, sample collection and analysis, decision to publish, or preparation of the manuscript.

References

Aneja VP, Isherwood A, Morgan P (2012) Characterization of particulate matter (PM10) related to surface coal mining operations in Appalachia. Atmos Environ 54:496–501. https://doi.org/10.1016/j.atmosenv.2012.02.063

ANLA (2015) Agreement No 0045 of January 22, 2015 (in Spanish). Colombian National Authority for Environmental Permits (ANLA for its acronym in Spanish). Ministry of Environment and Sustainable Development. Republic of Colombia. https://goo.gl/aouaed. Accessed 10 Oct 2017

Ashbaugh LL, Malm WC, Sadeh WZ (1985) A residence time probability analysis of sulfur concentrations at Grand Canyon National Park. Atmos Environ 19:1263–1270. https://doi.org/10.1016/0004-6981(85)90256-2

BP (2016) BP Statistical Review of World Energy June 2017, 66th edn. BP p.l.c., London. https://goo.gl/cWSxd3. Accessed 10 Oct 2017

Buseck PR, Jacob DJ, Posfai M, Li J, Anderson JR (2000) Minerals in the air: an environmental perspective. Int Geol Rev 42:577–593

Carslaw DC, Ropkins K (2012) openair—an R package for air quality data analysis. Environ Model Softw 27-28:52–61. https://doi.org/10.1016/j.envsoft.2011.09.008

Cerrejon (2016) Sustainability reports. Cerrejon's Division of Corporate Affairs and Communications. Bogota, Colombia. https://goo.gl/xM8QuZ. Accessed 2 Jan 2018

Chaulya SK (2004) Assessment and management of air quality for an opencast coal mining area. J Environ Manag 70:1–14. https://doi.org/10.1016/j.jenvman.2003.09.018

CIOH (2010) Climatology of the main ports of the Colombian Caribbean Riohacha (in Spanish). Colombian Center of Oceanographic and Hydrologic Research (CIOH for its acronym in Spanish). Republic of Colombia. Cartagena, Colombia. https://goo.gl/fgR3rS. Accessed 10 Oct 2017

CPCB (2003) Central Pollution Control Board. Ministry of Environment & Forests. Government of India. Printed at National Institute of Science Communication. Delhi, India. https://goo.gl/Y6kZhp. Accessed 10 Oct 2017

DANE (2005) General Census 2005 (in Spanish). National Administrative Department of Statistics (DANE for its acronym in Spanish). Republic of Colombia. https://goo.gl/sTo0Mp. Accessed 10 Oct 2017

DEE (2008) Air Quality Standards. Department of Environment and Energy. Australian Goverment. Canberra, Australia. https://goo.gl/5qpzsL. Accessed 19 Nov 2017

EIA (2017) International energy outlook 2017. Energy Information Administration. Energy Data & Statistics. United States of America Government. Washington, DC. https://goo.gl/ep8of5. Accessed 19 Nov 2017

EPA (1999) Reference Method for the Determination of Particulate Matter as PM10 in the Atmosphere. 40CFR50, Appendix J. United States of America Environmental Protection Agency. United States of America Government. Research Triangle Park, NC, USA. https://goo.gl/xNazLw. Accessed 19 Nov 2017

EPA (2011) Reference method for the determination of suspended particle matter in the atmosphere (high volume method). 40CFR50, Appendix B. United States of America Environmental Protection Agency. United States of America Government. Research Triangle Park, NC, USA. https://goo.gl/Cf4HTj. Accessed 19 Nov 2017

EPA (2017) Air Topics. United States of America Environmental Protection Agency. United States of America Government. Research Triangle Park, NC, USA. https://goo.gl/sbyu4S. Accessed 19 Nov 2017

Finkelman RB et al (2002) Health impacts of coal and coal use: possible solutions. Int J Coal Geol 50:425–443. https://doi.org/10.1016/s0166-5162(02)00125-8

George KV, Patil DD, Alappat BJ (2013) PM10 in the ambient air of Chandrapur coal mine and its comparison with other environments. Environ Monit Assess 185:1117–1128. https://doi.org/10.1007/s10661-012-2619-8

Ghose MK, Majee SR (2001) Air pollution caused by opencast mining and its abatement measures in India. J Environ Manag 63:193–202. https://doi.org/10.1006/jema.2001.0434

Ghose MK, Majee SR (2007) Characteristics of hazardous airborne dust around an Indian surface coal mining area. Environ Monit Assess 130:17–25. https://doi.org/10.1007/s10661-006-9448-6

Grantz DA, Garner JHB, Johnson DW (2003) Ecological effects of particulate matter. Environ Int 29:213–239. https://doi.org/10.1016/s0160-4120(02)00181-2

Kim KH, Kabir E, Kabir S (2015) A review on the human health impact of airborne particulate matter. Environ Int 74:136–143. https://doi.org/10.1016/j.envint.2014.10.005

Koçak M, Theodosi C, Zarmpas P, Im U, Bougiatioti A, Yenigun O, Mihalopoulos N (2011) Particulate matter (PM10) in Istanbul: origin, source areas and potential impact on surrounding regions. Atmos Environ 45:6891–6900. https://doi.org/10.1016/j.atmosenv.2010.10.007

Kunzli N et al (2000) Public-health impact of outdoor and traffic-related air pollution: a European assessment. Lancet 356:795–801. https://doi.org/10.1016/s0140-6736(00)02653-2

Lei YD, Wania F (2004) Is rain or snow a more efficient scavenger of organic chemicals? Atmos Environ 38:3557–3571. https://doi.org/10.1016/j.atmosenv.2004.03.039

Leiva MA, Santibanez DA, Ibarra ES, Matus CP, Seguel R (2013) A five-year study of particulate matter (PM2.5) and cerebrovascular diseases. Environ Pollut 181:1–6. https://doi.org/10.1016/j.envpol.2013.05.057

MADS (2010) Resolution number (610). Ministry of environment, housing and territorial development. Republic of Colombia. Bogota, Colombia. https://goo.gl/r3S8yB. Accessed 19 Nov 2017

Manzano CA et al (2016) Temporal variation in the deposition of polycyclic aromatic compounds in snow in the Athabasca Oil Sands area of Alberta. Environ Monit Assess 188:542. https://doi.org/10.1007/s10661-016-5500-3

Manzano CA, Marvin C, Muir D, Harner T, Martin J, Zhang Y (2017) Heterocyclic aromatics in petroleum coke, snow, lake sediments, and air samples from the Athabasca oil sands region. Environ Sci Technol 51(10):5445. https://doi.org/10.1021/acs.est.7b01345

Molina C, Toro R, Morales RGE, Manzano C, Leiva-Guzman MA (2017) Particulate matter in urban areas of south-central Chile exceeds air quality standards. Air Qual Atmos Health 10:653–667. https://doi.org/10.1007/s11869-017-0459-y

National Research Council N (2010) Global sources of local pollution: an assessment of long-range transport of key air pollutants to and from the United States. The National Academies Press, Washington, DC. https://doi.org/10.17226/12743

Oh HR et al (2015) Long-range transport of air pollutants originating in China: a possible major cause of multi-day high-PM10 episodes during cold season in Seoul, Korea. Atmos Environ 109:23–30. https://doi.org/10.1016/j.atmosenv.2015.03.005

Onder M, Yigit E (2009) Assessment of respirable dust exposures in an opencast coal mine. Environ Monit Assess 152:393–401. https://doi.org/10.1007/s10661-008-0324-4

QGIS (2016) QGIS Development Team. QGIS Geographic Information System. Open Source Geospatial Foundation Project. http://qgis.osgeo.org. Accessed 19 Nov 2017

Querol X et al (2004) Speciation and origin of PM10 and PM2.5 in selected European cities. Atmos Environ 38:6547–6555. https://doi.org/10.1016/j.atmosenv.2004.08.037

Rojano R (2015) Eficiencia en la reducción de emisiones de PM10 en un pit de una mina de carbón a cielo abierto. VIII Congreso Latinoamericano de Ciencias Ambientales. Sociedad de Química Ambiental de Chile, Pocun, p. 140

Rojano R, Arregoces H, Angulo LC, Restrepo G, Marin JM (2017) Factor and cluster analysis for PM10 concentrations in an open pit coal mine: Cerrejon, Colombia. Interciencia 42:44–50

Rolph G, Stein A, Stunder B (2017) Real-time environmental applications and display system: READY. Environ Model Softw 95:210. https://doi.org/10.1016/j.envsoft.2017.06.025

Salvador P et al (2016) Composition and origin of PM10 in Cape Verde: characterization of long-range transport episodes. Atmos Environ 127:326–339. https://doi.org/10.1016/j.atmosenv.2015.12.057

Song XY, Shao LY, Zheng QM, Yang SS (2014) Mineralogical and geochemical composition of particulate matter (PM10) in coal and non-coal industrial cities of Henan Province, North China. Atmos Res 143:462–472. https://doi.org/10.1016/j.atmosres.2014.03.015

Stein AF, Draxler RR, Rolph GD, BJB S, Cohen MD, Ngan F (2015) NOAA'S HYSPLIT atmospheric transport and dispersion modeling system. Bull Am Meteorol Soc 96:2059–2077. https://doi.org/10.1175/bams-d-14-00110.1

Tecer LH, Suren P, Alagha O, Karaca F, Tuncel G (2008) Effect of meteorological parameters on fine and coarse particulate matter mass concentration in a coal-mining area in Zonguldak. Turkey J Air Waste Manage Assoc 58:543–552. https://doi.org/10.3155/1047-3289.58.4.543

Tolis EI et al (2014) Chemical characterization of particulate matter (PM) and source apportionment study during winter and summer period for the city of Kozani. Greece Cent Eur J Chem 12:643–651. https://doi.org/10.2478/s11532-014-0531-5

Wang YQ (2014) MeteoInfo: GIS software for meteorological data visualization and analysis. Meteorol Appl 21:360–368. https://doi.org/10.1002/met.1345

Wang YQ, Zhang XY, Draxler RR (2009) TrajStat: GIS-based software that uses various trajectory statistical analysis methods to identify potential sources from long-term air pollution measurement data. Environ Model Softw 24:938–939. https://doi.org/10.1016/j.envsoft.2009.01.004

WCI (2005) The coal resource - a comprehensive overview of coal. World Coal Institute. World Coal Association. London, UK. https://goo.gl/BFoQkx. Accessed 19 Nov 2017

White AF, Blum AE (1995) Effects of climate on chemical-weathering in watersheds. Geochim Cosmochim Acta 59:1729–1747. https://doi.org/10.1016/0016-7037(95)00078-e

WHO (2006) Air quality guidelines - global update 2005. World Health Organization. Ginebra, Suiza. https://goo.gl/XQRNLZ. Accessed 19 Nov 2017

WHO (2016) Global urban ambient air pollution database - news release. World Health Organization. Ginebra, Suiza. https://goo.gl/ShiW8y. Accessed 10 Oct 2017

Xin YJ, Wang GC, Chen L (2016) Identification of long-range transport pathways and potential sources of PM10 in Tibetan Plateau uplift area: case study of Xining, China in 2014. Aerosol Air Qual Res 16:1044–1054. https://doi.org/10.4209/aaqr.2015.05.0296